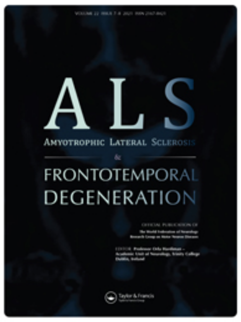

Amyotrophic Lateral Sclerosis and Frontotemporal Degeneration

ISSN: (Print) (Online) Journal homepage: https://www.tandfonline.com/loi/iafd20

Cerebellar degeneration in primary lateral sclerosis: an under-recognized facet of PLS

Eoin Finegan, We Fong Siah, Stacey Li Hi Shing, Rangariroyashe H. Chipika, Orla Hardiman & Peter Bede

Amyotrophic Lateral Sclerosis and Frontotemporal Degeneration, 2022; 0: 1–12

RESEARCH ARTICLE

Cerebellar degeneration in primary lateral sclerosis: an under-recognized facet of PLS

EOIN FINEGAN[1], WE FONG SIAH[1], STACEY LI HI SHING[1], RANGARIROYASHE H. CHIPIKA[1], ORLA HARDIMAN[1] & PETER BEDE[1,2]

[1]*Computational Neuroimaging Group, Biomedical Sciences Institute, Trinity College Dublin, Dublin, Ireland,* [2]*Department of Neurology, St James's Hospital Dublin, Dublin, Ireland*

Abstract

While primary lateral sclerosis (PLS) has traditionally been regarded as a pure upper motor neuron disorder, recent clinical, neuroimaging and postmortem studies have confirmed significant extra-motor involvement. Sporadic reports have indicated that in addition to the motor cortex and corticospinal tracts, the cerebellum may also be affected in PLS. Cerebellar manifestations are difficult to ascertain in PLS as the clinical picture is dominated by widespread upper motor neuron signs. The likely contribution of cerebellar dysfunction to gait disturbance, falls, pseudobulbar affect and dysarthria may be overlooked in the context of progressive spasticity. The objective of this study is the comprehensive characterization of cerebellar gray and white matter degeneration in PLS using multiparametric quantitative neuroimaging methods to systematically evaluate each cerebellar lobule and peduncle. Forty-two patients with PLS and 117 demographically-matched healthy controls were enrolled in a prospective MRI study. Complementary volumetric and voxelwise analyses revealed focal cerebellar alterations instead of global cerebellar atrophy. Bilateral gray matter volume reductions were observed in lobules III, IV and VIIb. Significant diffusivity alterations within the superior cerebellar peduncle indicate disruption of the main cerebellar outflow tracts. These findings suggest that the considerable intra-cerebellar disease-burden is coupled with concomitant cerebro-cerebellar connectivity disruptions. While cerebellar dysfunction is challenging to demonstrate clinically, cerebellar pathology is likely to be a significant contributor to disability in PLS.

Keywords: *Primary lateral sclerosis, Motor neuron disease, cerebellum, MRI, diffusion imaging, neuroimaging, clinical trials*

Introduction

Despite landmark contributions, detailed postmortem reports in PLS are scarce (1) and cerebellar involvement is seldom addressed. One case report described the cerebellum as "unremarkable" (2). This is in contrast to ALS, where TDP-43 immunopositive oligodendrocytes have been reported in cerebellar white matter (3) and neuroimaging studies have consistently confirmed cerebellar involvement (4–6). Despite the paucity of postmortem reports in PLS, imaging studies have indicated some degree of cerebellar involvement in vivo (7). The cerebellum is thought to be one of the most affected brain regions only outranked by corticospinal tract and corpus callosum degeneration (8). Cerebro-cerebellar functional connectivity alterations (9,10), cerebellar peduncle diffusivity changes (9,10), and spinocerebellar tract degeneration have been previously described (11). Marked brainstem atrophy has also been demonstrated in PLS, which may reflect loss of cerebellar connections (12,13). Cerebellar gray matter atrophy has been observed in PLS, but the predilection for specific cerebellar lobules is poorly characterized. Cerebellar changes are considered to be more pronounced in PLS compared with ALS, despite controlling for symptom duration (14). The extensive cerebellar involvement in PLS in comparison to ALS, even after adjustments for thelonger symptom duration, adds to the expanding evidence for divergent brain signatures between PLS and ALS (15). However, despite the compelling radiological evidence, frank cerebellar ataxia is seldom observed in PLS (10,11,16). Subtle cerebellar signs may be masked by the manifestations of severe corticospinal degeneration and systematic cerebellar assessments are not routinely performed in PLS, therefore the clinical impact of cerebellar

Correspondence: Professor Peter Bede, Computational Neuroimaging Group, Trinity Biomedical Sciences Institute, Trinity College Dublin, Room 5.43, Pearse Street, Dublin 2, Ireland. E-mail: bedep@tcd.ie

(Received 3 August 2021; revised 13 December 2021; accepted 17 December 2021)

DOI: 10.1080/21678421.2021.2023188

dysfunction is likely to be underestimated. The contribution of cerebellar pathology to poor balance and recurrent falls, a major cause of morbidity in PLS, is unknown, but is likely to be significant (16,17). Eye-movements abnormalities have been consistently described in ALS and are typically attributed to cerebellar pathology (18). Abnormal saccadic eye-movements are also described in PLS using eye-tacking methods (19). Cerebellar pathology may also contribute to cognitive deficits (20), bulbar impairment (21,22), respiratory compromise (23) and behavioral changes (24,25). Similar to ALS (26), executive dysfunction, language deficits, impaired verbal fluency and behavioral dysfunction have been consistently observed in PLS (8,27,28). Analogous to observations in ALS (29,30), deficits in social cognition are also increasingly recognized in PLS (31). While pseudobulbar affect (PBA) has traditionally been attributed to corticobulbar disconnection and lobe frontal pathology (32,33), the role of the cerebellum in the pathogenesis of PBA is increasingly recognized (34–38). Despite emerging clinical, post mortem and radiological evidence of cerebellar pathology in PLS (39), the predilection for specific cerebellar lobules and the preferential involvement of cerebellar peduncles have not been systematically evaluated in a large cohort of PLS patients (40). The comprehensive analysis of regional cerebellar involvement may help to bridge the gap between imaging and clinical observations and provide further insights into the phenotype-specific pathological patterns (41). The objective of this study is the characterization of lobule-wise cerebellar gray matter profiles in PLS, complemented by region-of-interest morphometric, diffusivity, and cerebellar peduncle integrity analyses.

Methods

Participants

Forty-two patients with PLS were recruited in this prospective neuroimaging study, diagnosed according to the new consensus diagnostic criteria (42). MRI data from 117 demographically-matched healthy controls were used for the interpretation of their imaging data. Healthy controls were unrelated to the participating PLS patients and had no established neurological or psychiatric diagnoses. The study was approved by the Ethics Committee of Beaumont Hospital, Dublin, Ireland and all participants provided informed consent prior to inclusion.

Magnetic resonance imaging

T1-weighted images were acquired on a 3 Tesla Philips Achieva system using a 3D Inversion Recovery prepared Spoiled Gradient Recalled echo (IR-SPGR) pulse sequence and an 8-channel receive-only head coil. The following pulse sequence settings were implemented; field-of-view (FOV): $256 \times 256 \times 160$ mm, slice orientation: sagittal, spatial resolution: 1 mm^3, TR/TE = 8.5/3.9 ms, TI =1060 ms, flip angle = 8°, SENSE factor = 1.5. 32-direction DTI images were recorded using a spin-echo echo planar imaging (SE-EPI) pulse sequence with the following parameters: TR/TE = 7639/59 ms, slice orientation: transverse (axial), SENSE factor = 2.5, b-values = 0, 1100s/mm^2 FOV = $245 \times 245 \times 150$ mm, spatial resolution = 2.5 mm^3, 60 slices were acquired with no interslice gaps. Fluid attenuated inversion recovery (FLAIR) images were also acquired for each participant to rule out alternative or comorbid pathologies and assess for vascular white matter lesion burden. FLAIR images were acquired using an Inversion Recovery Turbo Spin Echo (IR-TSE) sequence in axial orientation: TR/TE = 11000/125 ms, TI = 2800 ms, 120° refocusing pulse, FOV = $230 \times 183 \times 150$ mm, spatial resolution = $0.65 \times 0.87 \times 4$ mm, 30 slices with 1 mm gap, with flow compensation and motion smoothing and a saturation slab covering the neck region. Imaging data were evaluated in voxelwise analyses, based on lobular volume and region-of-interest peduncle diffusivity profiles.

Voxelwise gray matter analyses

Total intracranial volumes (TIV) were calculated for each subject to be used as a covariate in subsequent morphometric analyses. As described in detail previously (12,43), TIV was estimated by linearly aligning each participant's skull-stripped brain image to the MNI152 standard, and the inverse of the determinant of the affine registration matrix was calculated and multiplied by the size of the template. FMRIB's FSL-FLIRT was utilized for spatial registration and FSL-FAST for tissue segmentation. TIV was calculated by the addition of partial-volume gray matter, white matter and CSF volumes. FMRIB's FSL (44,45) was used for voxelwise morphometry. The pre-processing steps included skull-removal and tissue-type segmentation which were individually verified for each subject. Using the standard FMIRB pipeline, partial-volume gray-matter data were aligned to MNI152 standard space and a study-specific GM template was created to which the gray matter images from each participant were co-registered (45). To evaluate cerebellar gray matter changes in PLS compared to healthy controls, permutation based non-parametric inference was implemented using the threshold-free cluster enhancement (TFCE) method. The design matrix included study group membership and the relevant demeaned covariates; age, gender and total intracranial volumes. Voxelwise analyses were restricted to the cerebellum as defined by "label 1" of the MNI structural atlas. Resulting statistical outputs were thresholded at $p < 0.01$ FWE/TFCE and the Diedrichsen probabilistic atlas was used as underlay to present the localization of statistically significant clusters (46).

Cerebellar tract-wise white matter analyses

Raw diffusion data first underwent eddy current corrections and skull removal (47) before a tensor model was fitted to generated maps of fractional anisotropy (FA) and radial diffusivity (RD). The standard FMRIB's Tract-based Statistics pipeline was used for non-linear registration, skeletonization of FA images, creation of a study-specific mean FA mask and also for the registration and skeletonization of RD images (48). Permutation-based non-parametric statistics was used to characterize the voxelwise diffusivity profile of PLS patients in contrast to healthy controls. Covariates included age and gender. The threshold-free cluster enhancement (TFCE) approach was implemented and resulting outputs were thresholded at $p < 0.01$ corrected for family-wise error (FWE).

Cerebellar lobule volumetry

The cerebellum was parcellated using a multi-atlas segmentation approach (49). The pre-processing steps included T1w data "denoising" in native space, corrections for inhomogeneity, affine registration to Montreal Neurological Institute (MNI) space, inhomogeneity corrections in MNI space, cerebellar cropping, low dimensional non-linear registration estimation, and intensity normalization. A patch-based parcellation algorithm was implemented to generate cerebellar volume metrics for each lobule in each hemisphere (50). As a quality control step, anatomical segmentation and tissue-type parcellation accuracy was individually checked for each subject. Volumetric values were extracted for the following structures: Lobules I-II, III, IV, V, VI, VIIB, VIIIA, VIIIB, IX, X, Crus I and Crus II. Following verification of data assumptions, analysis of covariance (ANCOVA) was performed to compare the cerebellar profile of PLS patients to controls with the following covariates: total intracranial volume, age and sex.

Cerebellar peduncles

The integrity of the cerebellar peduncles was assessed in region-of-interest (ROI) analyses. The relevant labels of the 1mm JHU-ICBM atlas were used to generate masks for inferior (ICP), middle (MCP) and superior cerebellar peduncles (SCP). As per the original atlas, separate right and left labels were used for the inferior and superior peduncles and a single label generated for the middle cerebellar peduncle. Average FA and RD values were then extracted from the merged skeletonized diffusion data using these anatomical masks for subsequent statistical analyses. ANCOVA was used to contrast the diffusivity values in the cerebellar peduncles in PLS patients to healthy controls using age and sex as covariates.

Results

The PLS cohort (mean age: 60.95 ± 9.7, 27 males) and healthy controls (mean age: 63.7 ± 8.2, 70 males) were matched for age ($p = 0.079$), gender ($\chi 2 = 0.105$, $p = 0.74$), education ($p = 0.27$) and handedness ($\chi 2 = 0.051$, $p = 0.822$).

Voxelwise findings

Voxelwise gray matter analysis identified bilateral morphometric changes in lobules V, VI and VIIIb as well as in Crus 1. Alterations were largely symmetric with slight right-sided predominance (Figure 1).

Symmetric white matter degeneration was detected by tract-wise analyses. FA reductions were detected in lobules I-IV, V, VI, and in the bilateral inferior and superior cerebellar peduncles and in the vermis at $p < 0.01$ FWE (Figure 2). Increased RD was detected in the middle and superior cerebellar peduncles, in Crus II, the vermis and lobule VI at $p < 0.01$ FWE (Figure 3).

Cerebellar lobule volumes

Total cerebellar gray matter volume was significantly reduced bilaterally in the PLS group in comparison with controls. At a lobule-level, significant bilateral gray matter volume reductions were identified in lobules III, IV and VIIB, while significant reductions were also identified in Crus II (left) and VIIIA (right) (Table 1). To highlight the preferential atrophy of specific lobules, the age-, sex- and TIV-corrected estimated marginal means of cerebellar lobule volumes were plotted in radar plots with reference to the control data defined as 100% (Figure 4).

Cerebellar peduncle integrity

Fractional anisotropy reductions were identified in the bilateral inferior cerebellar peduncles. Increased bihemispheric radial diffusivity was detected in the superior and inferior cerebellar peduncles (Table 2).

Discussion

The dedicated analysis of cerebellar disease burden in PLS confirms selective cerebellar lobule involvement in PLS. The greatest volume loss was identified in lobules III, IV and VIIb bilaterally. Our findings point to focal instead of global cerebellar

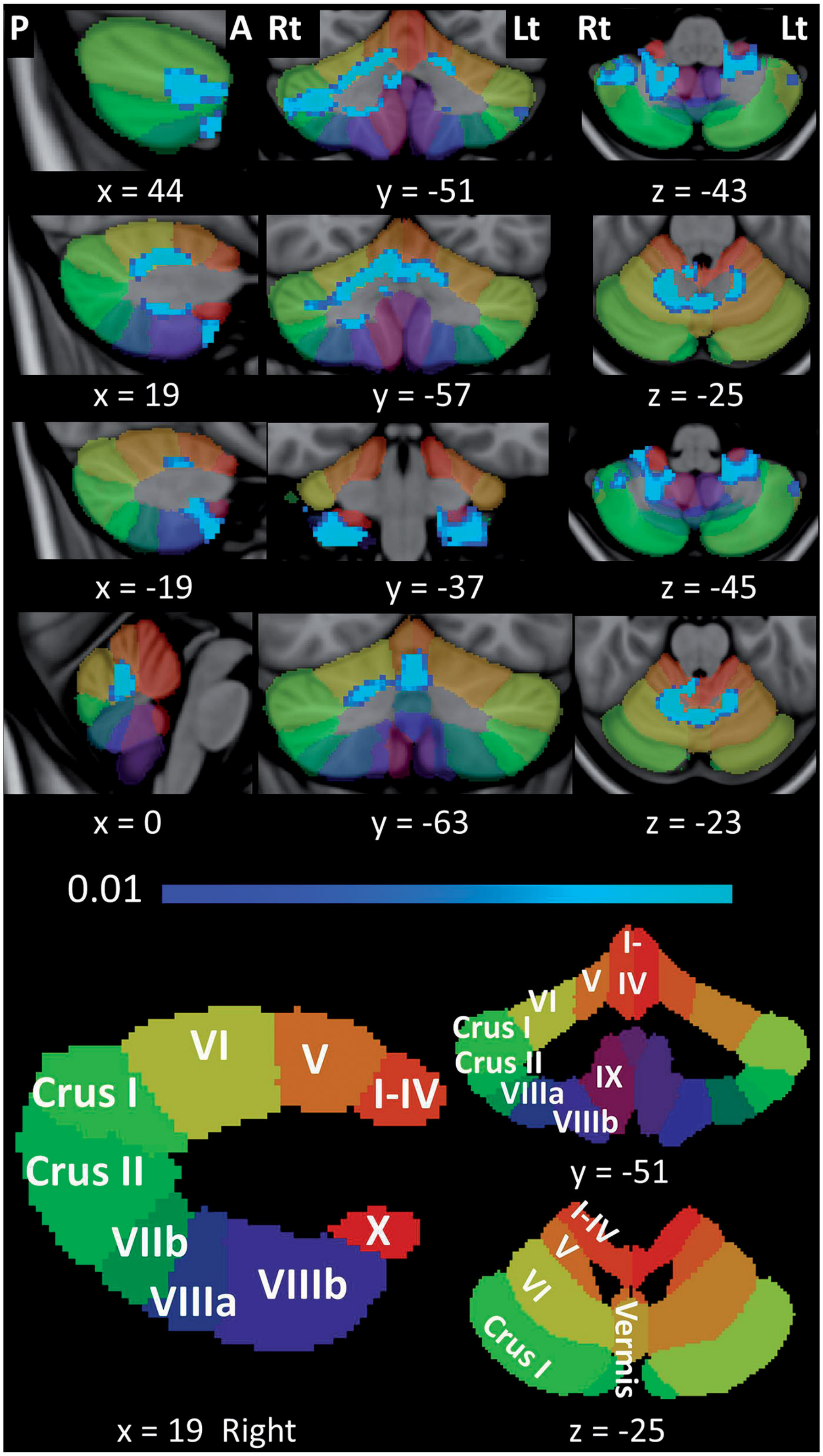

Figure 1. Patterns of cerebellar gray matter atrophy in PLS are shown in blue color with reference to healthy controls at $p < 0.01$ FWE corrected for age, sex and TIV. MNI coordinates are provided for sagittal (x), coronal (y) and axial views (z). The Diedrichsen probabilistic cerebellar atlas is presented as underlay to aid localization. The anatomical labels of atlas are presented at the bottom. Radiological convention used, P – Posterior, A – Anterior, Lt – Left, Rt – Right.

degeneration in PLS, and demonstrate that intra-cerebellar pathology is accompanied by cerebellar peduncle degeneration. From a functional anatomy perspective, the anterior lobe of the cerebellum (lobules I-V), along with the adjacent lobule VI are predominantly associated with cerebellar motor function (24), whereas the posterior lobe is classically linked to cognitive and affective functions (25). Within the cerebellar hemispheres, white matter pathology showed a predilection for the

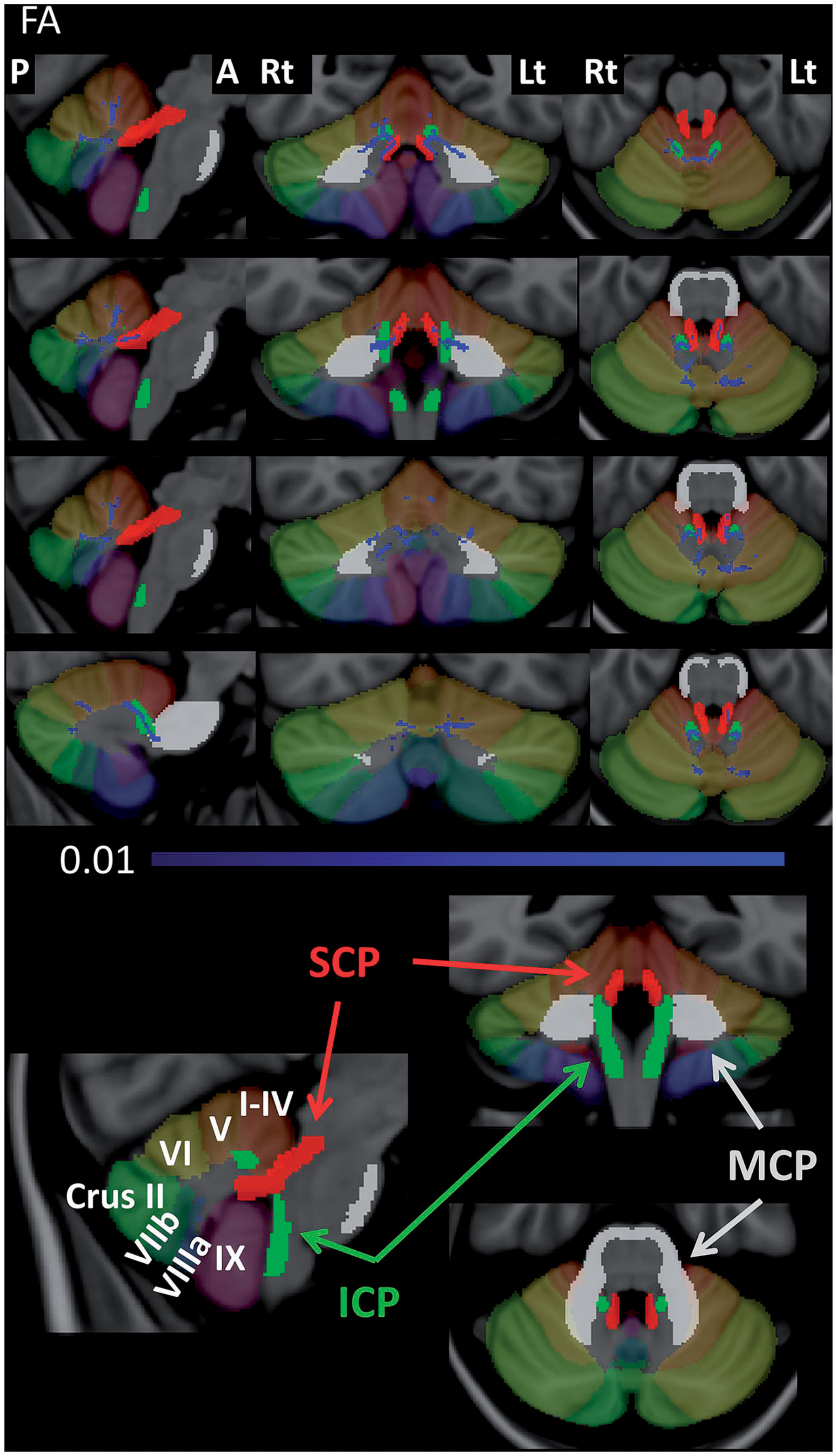

Figure 2. Patterns of fractional anisotropy reductions in PLS are presented in blue color with reference to healthy controls at $p < 0.01$ FWE corrected for age and sex. The Diedrichsen probabilistic cerebellar atlas and the superior cerebellar peduncle (SCP – red), middle cerebellar peduncle (MCP – white) and inferior cerebellar peduncle (ICP – green) labels of the ICBM-DTI-81 white-matter atlas are presented as underlay to aid localization. The anatomical labels of atlases are presented at the bottom. Radiological convention used, P – Posterior, A – Anterior, Lt – Left, Rt – Right. The MNI coordinates of the views in the four rows are the following (x/y/z): 5/-50/-22, 6/-45/-26, 5/-59/-27, -12/-66/-25.

anterior lobes with the preferential involvement lobules III, IV and V, as well as the adjacent lobule VI, within the posterior lobe. Gray matter involvement was more widespread throughout the cerebellum. Both gray and white matter atrophy was identified in lobules III and IV, bilaterally. Multiple studies have linked pathology in these lobules to gait ataxia (51,52). Similarly, converging

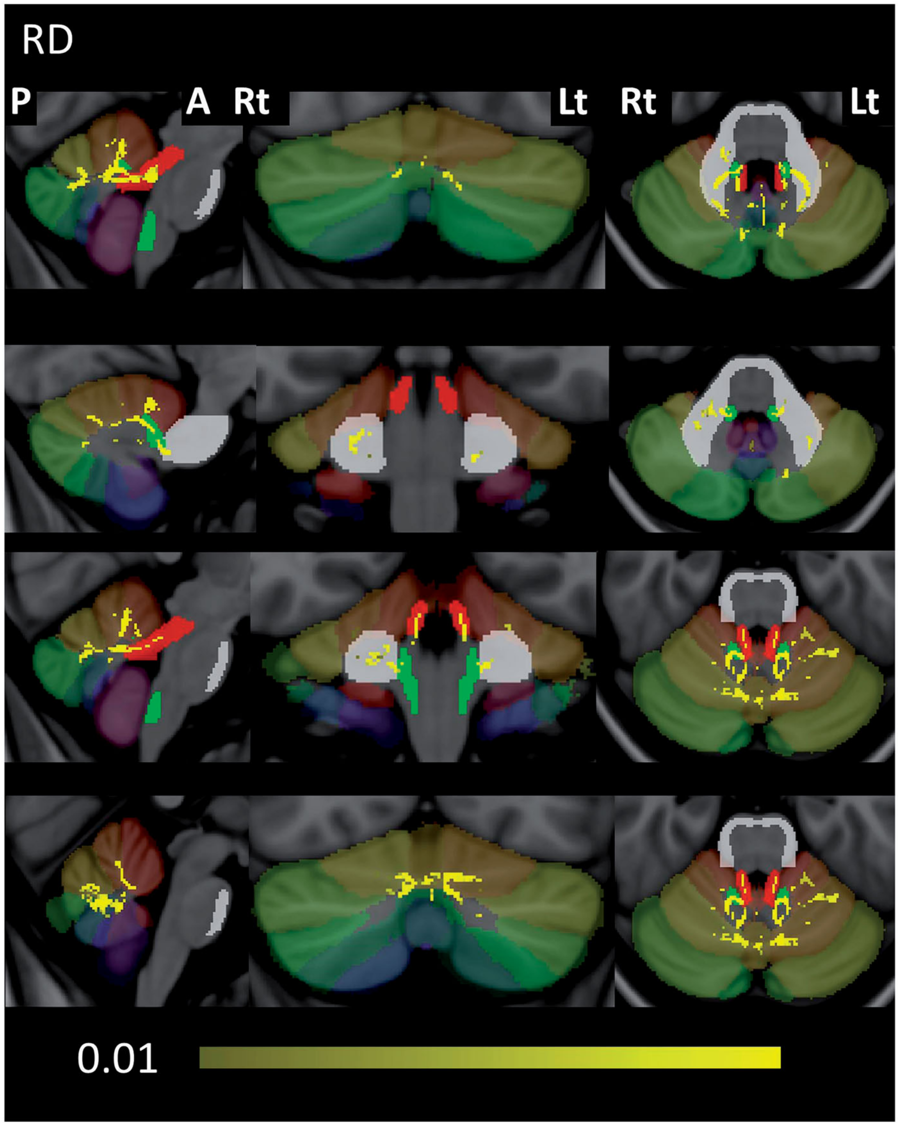

Figure 3. Patterns of increased radial diffusivity in PLS are shown in yellow color with reference to healthy controls at $p < 0.01$ FWE corrected for age and sex. The Diedrichsen probabilistic cerebellar atlas and the superior cerebellar peduncle (SCP – red), middle cerebellar peduncle (MCP – white) and inferior cerebellar peduncle (ICP – green) labels of the ICBM-DTI-81 white-matter atlas are presented as underlay to aid localization. Radiological convention used, P – Posterior, A – Anterior, Lt – Left, Rt – Right. The MNI coordinates of the views in the four rows are the following (x/y/z): 7/-72/-32, -12/-37/-37, 6/-40/-26, -1/-68/-26.

evidence attributes cerebellar dysarthria to involvement of lobules V and VI, both of which showed significant bilateral white matter alterations in our PLS cohort (25,51).

While cerebellar motor regions were significantly affected on volumetric, diffusivity and voxel-based gray matter analyses, results were less concordant in lateral regions which are particularly linked to cognitive function such as Crus I and Crus II. Mild, significant volume loss was detected in Crus II in the left hemisphere only (53). Similarly, lobule IX integrity, implicated in cerebellar cognitive function did not differ significantly from healthy controls on any metric (25,52,53).

The analyses of white matter diffusion metrics highlight the involvement of the cerebellar peduncles. The superior, middle, and inferior cerebellar peduncles provide the structural connection between the cerebellum and the brainstem. Our region-of-interest diffusivity analyses confirmed increased RD in the bilateral superior and inferior cerebellar peduncles and FA reductions in the inferior cerebellar peduncles. Additionally, our voxelwise analyses detected radial diffusivity alterations in the middle cerebellar peduncles. The superior cerebellar peduncles are the primary output tracts of the cerebellum connecting the cerebellar nuclei to the contralateral cortex via the ventral lateral nuclei, although they also contain spinocerebellar afferents (54,55). It is noteworthy, that the ventral lateral thalamic nuclei have previously been found to be affected in PLS (56,57). Superior cerebellar peduncle involvement has been described in a previous study of 3 PLS patients, in whom significantly lower FA was recorded in comparison with controls (58). Cerebellar peduncle

Table 1. Cerebellar lobule gray matter volumes in PLS and controls adjusted for age, sex, total intracranial volumes.

Cerebellar region	Study group	Estimated marginal mean	Standard error	ANCOVA Sig. (*p*)
Total Cerebellum (right)	HC	47.721702	0.369059	**.019***
	PLS	45.955560	0.630152	
Total Cerebellum (left)	HC	47.669366	0.361897	**.009***
	PLS	45.733854	0.617924	
Lobules I–II (right)	HC	0.034246	0.000866	.754
	PLS	0.033698	0.001478	
Lobules I–II (left)	HC	0.029409	0.000968	.294
	PLS	0.027353	0.001653	
Lobule III (right)	HC	0.492044	0.009323	**.016***
	PLS	0.446228	0.015919	
Lobule III (left)	HC	0.501364	0.010294	**.037***
	PLS	0.457689	0.017577	
Lobule IV (right)	HC	1.936520	0.026081	**<.001***
	PLS	1.746658	0.044531	
Lobule IV (left)	HC	2.071227	0.030074	**.001***
	PLS	1.867074	0.051350	
Lobule V (right)	HC	3.289151	0.042784	.077
	PLS	3.135760	0.073051	
Lobule V (left)	HC	3.566098	0.042539	.113
	PLS	3.429295	0.072633	
Lobule VI (right)	HC	7.847142	0.098904	.174
	PLS	7.574638	0.168875	
Lobule VI (left)	HC	7.870016	0.096677	.153
	PLS	7.589976	0.165071	
Crus I (right)	HC	11.080734	0.147747	.912
	PLS	11.047597	0.252272	
Crus I (left)	HC	11.080363	0.153723	.266
	PLS	10.734727	0.262475	
Crus II (right)	HC	7.067282	0.108867	.081
	PLS	6.681765	0.185886	
Crus II (left)	HC	6.901220	0.100807	**.043***
	PLS	6.487647	0.172123	
Lobule VIIB (right)	HC	4.207641	0.058063	**<.001***
	PLS	3.786151	0.099140	
Lobule VIIB (left)	HC	4.035672	0.056800	**<.001***
	PLS	3.603847	0.096983	
Lobule VIIIA (right)	HC	4.831938	0.057846	**.030***
	PLS	4.576008	0.098769	
Lobule VIIIA (left)	HC	4.901696	0.061875	.412
	PLS	4.799118	0.105648	
Lobule VIIIB (right)	HC	3.395932	0.059408	.801
	PLS	3.426117	0.101437	
Lobule VIIIB (left)	HC	3.317364	0.050465	.633
	PLS	3.366015	0.086167	
Lobule IX (right)	HC	2.832671	0.044305	.794
	PLS	2.809288	0.075648	
Lobule IX (left)	HC	2.668338	0.044368	.904
	PLS	2.657517	0.075756	
Lobule X (right)	HC	0.581185	0.006670	.501
	PLS	0.572123	0.011390	
Lobule X (left)	HC	0.582141	0.006502	.705
	PLS	0.577179	0.011101	

white matter abnormalities have been consistently reported in ALS (59–61) and linked to impaired cerebro-cerebellar connectivity, including projections to the primary and supplementary motor cortices (59). MCP integrity changes have also been consistently described in ALS (59,62). The involvement of the MCP has been demonstrated in PLS patients and has been linked to pseudobulbar affect (PBA), supporting the concept of cerebellar deafferentation in the pathogenesis of PBA (35).

The identification of selective cerebellar atrophy raises important clinical questions. The appreciation of subtle cerebellar signs in PLS is likely to be confounded by the marked upper motor neuron signs dominating the clinical landscape of PLS. The contribution of cerebellar dysfunction to gait disturbance, falls, dysarthria and dysphagia needs to be carefully considered in multidisciplinary interventions. The recognition that, similar to ALS (63,64), extra-pyramidal and cerebellar dysfunction may also contribute to motor disability in PLS

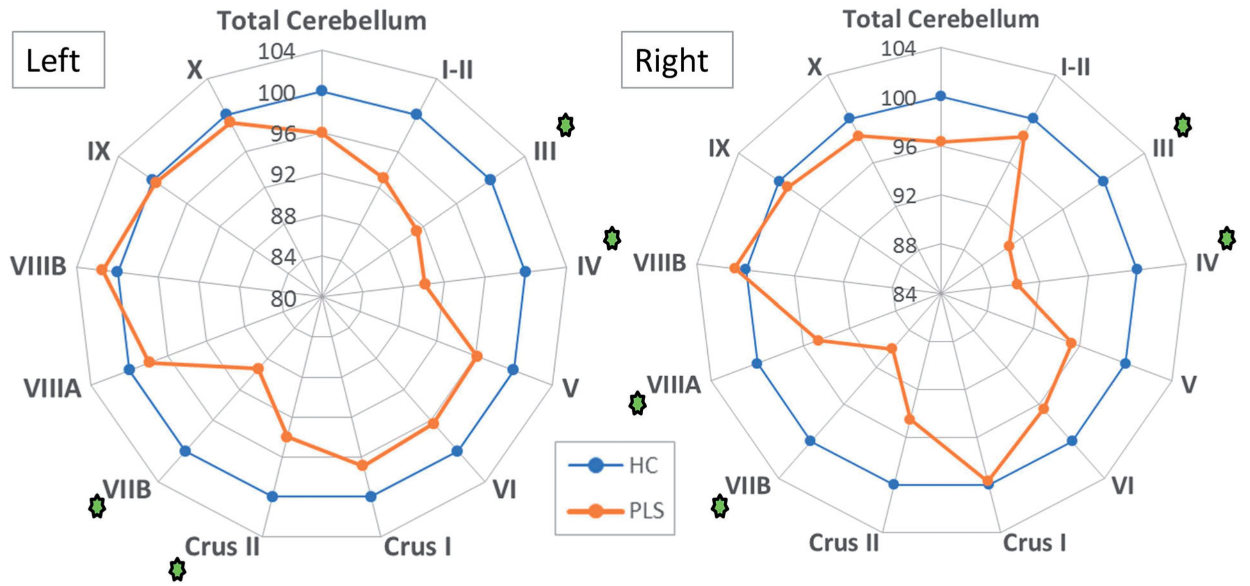

Figure 4. Selective cerebellar lobule degeneration in PLS. Age-, sex- and total intracranial volume corrected estimated marginal means of cerebellar lobule volumes are plotted in both hemispheres in radar plots with reference to the control data defined as 100%. Significant volumetric differences are flagged with a green star.

Table 2. Cerebellar peduncle integrity adjusted for age, gender.

Region	Study group	Estimated marginal mean	Standard error	ANCOVA Sig. (*p*)
Fractional Anisotropy (FA)				
Superior peduncle (left)	HC	0.624722	0.003738	.209
	PLS	0.615415	0.006293	
Superior peduncle (right)	HC	0.615139	0.003796	.246
	PLS	0.606419	0.006391	
Middle peduncle	HC	0.516641	0.003052	.754
	PLS	0.514754	0.005139	
Inferior peduncle (left)	HC	0.509868	0.003437	.056
	PLS	0.496806	0.005787	
Inferior peduncle (right)	HC	0.505411	0.003694	**.004***
	PLS	0.484106	0.006220	
Radial Diffusivity (RD)				
Superior peduncle (left)	HC	0.000452	0.000005	**.012***
	PLS	0.000477	0.000009	
Superior peduncle (right)	HC	0.000469	0.000005	**.044***
	PLS	0.000490	0.000009	
Middle peduncle	HC	0.000441	0.000003	.468
	PLS	0.000446	0.000006	
Inferior peduncle (left)	HC	0.000472	0.000004	**.017***
	PLS	0.000492	0.000007	
Inferior peduncle (right)	HC	0.000476	0.000004	**.002***
	PLS	0.000503	0.000007	
	PLS	0.000701	0.000007	

Bold p-values with asterisk indicate statistically significant changes.

(65) has potential implications for rehabilitation efforts, fall prevention and individualized occupational- and physio-therapy. The nuanced characterization of PLS-specific cerebellar signatures may also aid the development of classification algorithms in MND to correctly categorize early-stage patients into diagnostic and prognostic categories (66–70).

The chronology of cerebral and cerebellar degeneration in PLS is currently unclear as there is a scarcity of published longitudinal imaging studies in PLS (71–73). However, longitudinal ALS studies suggest that progressive cerebellar degeneration may be a relatively late feature (74–76). Functional studies of ALS (77,78) have postulated that the cerebellum may temporarily compensate for the degeneration of the primary motor cortex, but this has not been confirmed by post mortem and high-resolution structural studies (4,79). Increased cerebellar gray matter volume and increased white matter organization have been described in adult poliomyelitis survivors which were interpreted as putative compensatory adaptation to spinal cord insult in infancy (80,81).

Despite the contribution of emerging functional modalities such as EEG and MEG to MND research (78,82,83), these methods typically only acquire and analyze supratentorial data. Similarly, while wet biomarkers may be sensitive in tracking progressive neurodegenerative change in various MND phenotypes (84–86), these are anatomically nonspecific and provide no additional information relating to cerebellar change. Infratentorial imaging and targeted post mortem assessments are currently the two viable approaches to characterize infratentorial disease burden patterns in PLS.

This study is not without limitations. The cross-sectional design precludes the assessment of the chronology of cerebral and cerebellar degeneration and its relationship with symptom duration. Longitudinal studies are required to elucidate the timeline of infratentorial degeneration and verify putative compensatory processes. We used the ICBM152 template to register our structural data to MNI standard space, but the new spatially unbiased infra-tentorial template (SUIT) promises to preserve the anatomical detail of the cerebellum to a higher degree (87). Finally, pathological validation is required to uncover the cellular and subcellular hallmarks of cerebellar degeneration in PLS.

Conclusions

PLS is associated with considerable cerebellar gray and white matter degeneration with the preferential involvement of specific cerebellar lobules. Cerebellar pathology in PLS is likely to contribute to the heterogeneity of manifestations observed clinically. PLS should no longer be solely associated with pyramidal tract and motor cortex degeneration given the compelling evidence of concomitant extra-motor, extra-pyramidal and cerebellar pathology.

Acknowledgments

We thank all participating patients and each healthy control for supporting this research study. Without their contribution this study would not have been possible. We also express our gratitude to the caregivers and family members of participating patients for facilitating attendance at our neuroimaging centre. We also thank all patients who had expressed interest in this research study, but could not participate due to medical or logistical reasons.

Funding

This study was sponsored by the Spastic Paraplegia Foundation, Inc. (SPF). Professor Peter Bede and the Computational Neuroimaging Group are also supported by the Health Research Board (HRB EIA-2017-019), the EU Joint Programme – Neurodegenerative Disease Research (JPND), the Andrew Lydon scholarship, the Irish Institute of Clinical Neuroscience (IICN), and the Iris O'Brien Foundation.

Ethics Approval

This study was approved by the Ethics (Medical Research) Committee—Beaumont Hospital, Dublin, Ireland.

Author Contribution

Conceptualization of the study: EF, PB.
Drafting the manuscript: EF, PB.
Neuroimaging analyses: WFS, PB.
Revision of the manuscript for intellectual content: EF, WFS, SLHS, RHC, OH, PB.

References

1. Mackenzie IRA, Briemberg H. TDP-43 pathology in primary lateral sclerosis. Amyotroph Lateral Scler Frontotemporal Degener. 2020;21:52–8.
2. Tan C-F, Kakita A, Piao Y-S, Kikugawa K, Endo K, Tanaka M, et al. Primary lateral sclerosis: a rare upper-motor-predominant form of amyotrophic lateral sclerosis often accompanied by frontotemporal lobar degeneration with ubiquitinated neuronal inclusions? Report of an autopsy case and a review of the literature. Acta Neuropathol. 2003;105:615–20.
3. Brettschneider J, Del Tredici K, Toledo JB, Robinson JL, Irwin DJ, Grossman M, et al. Stages of pTDP-43 pathology in amyotrophic lateral sclerosis. Ann Neurol. 2013;74:20–38.
4. Prell T, Grosskreutz J. The involvement of the cerebellum in amyotrophic lateral sclerosis. Amyotroph Lateral Scler Frontotemporal Degener. 2013;14:507–15.
5. Bede P, Chipika RH, Christidi F, Hengeveld JC, Karavasilis E, Argyropoulos GD, et al. Genotype-associated cerebellar profiles in ALS: focal cerebellar pathology and cerebro-cerebellar connectivity alterations. J Neurol Neurosurg Psychiatry. 2021;92:1197–205.
6. Pizzarotti B, Palesi F, Vitali P, Castellazzi G, Anzalone N, Alvisi E, et al. Frontal and cerebellar atrophy supports FTSD-ALS clinical continuum. Front Aging Neurosci. 2020;12:593526.
7. Canu E, Agosta F, Galantucci S, Chiò A, Riva N, Silani V, et al. Extramotor damage is associated with cognition in primary lateral sclerosis patients. PLoS One. 2013;8:e82017.
8. Finegan E, Shing SLH, Chipika RH, Chang KM, McKenna MC, Doherty MA, et al. Extra-motor cerebral changes and manifestations in primary lateral sclerosis. Brain Imaging Behav 2021;15:2283–96.
9. Agosta F, Galantucci S, Riva N, Chiò A, Messina S, Iannaccone S, et al. Intrahemispheric and interhemispheric structural network abnormalities in PLS and ALS. Hum Brain Mapp. 2014;35:1710–22.
10. Meoded A, Morrissette AE, Katipally R, Schanz O, Gotts SJ, Floeter MK. Cerebro-cerebellar connectivity is increased in primary lateral sclerosis. Neuroimage Clin. 2015;7:288–96.
11. Tu S, Menke RAL, Talbot K, Kiernan MC, Turner MR. Cerebellar tract alterations in PLS and ALS. Amyotroph Lateral Scler Frontotemporal Degener. 2019;20:281–4.

12. Bede P, Chipika RH, Finegan E, Li Hi Shing S, Doherty MA, Hengeveld JC, et al. Brainstem pathology in amyotrophic lateral sclerosis and primary lateral sclerosis: a longitudinal neuroimaging study. Neuroimage Clin. 2019;24:102054.
13. Bede P, Chipika RH, Finegan E, Li Hi Shing S, Chang KM, Doherty MA, et al. Progressive brainstem pathology in motor neuron diseases: imaging data from amyotrophic lateral sclerosis and primary lateral sclerosis. Data Brief. 2020;29:105229.
14. Finegan E, Chipika RH, Li Hi Shing S, Doherty MA, Hengeveld JC, Vajda A, et al. The clinical and radiological profile of primary lateral sclerosis: a population-based study. J Neurol. 2019;266:2718–33.
15. Finegan E, Chipika RH, Doherty MA, et al. Primary lateral sclerosis, part of the MND spectrum or distinct entity: a multiparametric neuroimaging study with comprehensive clinical and genetic profiling. Amyotroph Lateral Scler Frontotemporal Degener 2018;19:11–2.
16. Barohn RJ, Fink JK, Heiman-Patterson T, Huey ED, Murphy J, Statland JM, et al. The clinical spectrum of primary lateral sclerosis. Amyotroph Lateral Scler Frontotemporal Degener. 2020;21:3–10.
17. Floeter MK, Warden D, Lange D, Wymer J, Paganoni S, Mitsumoto H. Clinical care and therapeutic trials in PLS. Amyotroph Lateral Scler Frontotemporal Degener. 2020; 21:67–73.
18. Donaghy C, Thurtell MJ, Pioro EP, Gibson JM, Leigh RJ. Eye movements in amyotrophic lateral sclerosis and its mimics: a review with illustrative cases. J Neurol Neurosurg Psychiatry. 2011;82:110–6.
19. Proudfoot M, Menke RAL, Sharma R, Berna CM, Hicks SL, Kennard C, et al. Eye-tracking in amyotrophic lateral sclerosis: a longitudinal study of saccadic and cognitive tasks. Amyotroph Lateral Scler Frontotemporal Degener. 2015;17: 101–11.
20. Malm J, Kristensen B, Karlsson T, Carlberg B, Fagerlund M, Olsson T. Cognitive impairment in young adults with infratentorial infarcts. Neurology 1998;51:433–40.
21. Yunusova Y, Plowman EK, Green JR, Barnett C, Bede P. Clinical measures of bulbar dysfunction in ALS. Front Neurol. 2019;10:106.
22. Sasegbon A, Hamdy S. The role of the cerebellum in swallowing. Dysphagia 2021. doi: 10.1007/s00455-021-10271-x
23. Xu F, Frazier DT. Role of the cerebellar deep nuclei in respiratory modulation. Cerebellum. 2002;1:35–40.
24. Stoodley CJ, Schmahmann JD. Functional topography in the human cerebellum: a meta-analysis of neuroimaging studies. Neuroimage. 2009;44:489–501.
25. Argyropoulos GPD, van Dun K, Adamaszek M, Leggio M, Manto M, Masciullo M, et al. The cerebellar cognitive affective/schmahmann syndrome: a task force paper. Cerebellum. 2020;19:102–25.
26. Christidi F, Karavasilis E, Rentzos M, Kelekis N, Evdokimidis I, Bede P. Clinical and radiological markers of extra-motor deficits in amyotrophic lateral sclerosis. Front Neurol. 2018;9:1005.
27. de Vries BS, Rustemeijer LMM, Bakker LA, Schröder CD, Veldink JH, van den Berg LH, et al. Cognitive and behavioural changes in PLS and PMA: challenging the concept of restricted phenotypes. J Neurol Neurosurg Psychiatry. 2019;90:141–7.
28. Le Forestier N, Maisonobe T, Piquard A, Rivaud S, Crevier-Buchman L, Salachas F, et al. Does primary lateral sclerosis exist? A study of 20 patients and a review of the literature. Brain. 2001;124:1989–99.
29. Burke T, Pinto-Grau M, Lonergan K, Elamin M, Bede P, Costello E, et al. Measurement of social cognition in amyotrophic lateral sclerosis: a population based study. PLoS One. 2016;11:e0160850.
30. Burke T, Elamin M, Bede P, Pinto-Grau M, Lonergan K, Hardiman O, et al. Discordant performance on the 'reading the mind in the eyes' test, based on disease onset in amyotrophic lateral sclerosis. Amyotroph Lateral Scler Frontotemporal Degener 2016;17:1–6.
31. de Vries BS, Spreij LA, Rustemeijer LMM, Bakker LA, Veldink JH, van den Berg LH, et al. A neuropsychological and behavioral study of PLS. Amyotroph Lateral Scler Frontotemporal Degener. 2019;20:376–84.
32. Hübers A, Kassubek J, Grön G, Gorges M, Aho-Oezhan H, Keller J, et al. Pathological laughing and crying in amyotrophic lateral sclerosis is related to frontal cortex function. J Neurol. 2016;263:1788–95.
33. Bede P, Finegan E. Revisiting the pathoanatomy of pseudobulbar affect: mechanisms beyond corticobulbar dysfunction. Amyotroph Lateral Scler Frontotemporal Degener. 2018;19:4–6.
34. Parvizi J, Anderson SW, Martin CO, Damasio H, Damasio AR. Pathological laughter and crying: a link to the cerebellum. Brain. 2001;124:1708–19.
35. Floeter MK, Katipally R, Kim MP, Schanz O, Stephen M, Danielian L, et al. Impaired corticopontocerebellar tracts underlie pseudobulbar affect in motor neuron disorders. Neurology 2014;83:620–7.
36. Finegan E, Chipika RH, Li Hi Shing S, Hardiman O, Bede P. Pathological crying and laughing in motor neuron disease: pathobiology, screening, intervention. Front Neurol. 2019;10:260.
37. Argyropoulos GD, Christidi F, Karavasilis E, Velonakis G, Antoniou A, Bede P, et al. Cerebro-cerebellar white matter connectivity in bipolar disorder and associated polarity subphenotypes. Prog Neuropsychopharmacol Biol Psychiatry. 2021;104:110034.
38. Christidi F, Karavasilis E, Ferentinos P, Xirou S, Velonakis G, Rentzos M, et al. Investigating the neuroanatomical substrate of pathological laughing and crying in amyotrophic lateral sclerosis with multimodal neuroimaging techniques. Amyotroph Lateral Scler Frontotemporal Degener 2017;19:1–9.
39. Pioro EP, Turner MR, Bede P. Neuroimaging in primary lateral sclerosis. Amyotroph Lateral Scler Frontotemporal Degener. 2020;21:18–27.
40. Bede P, Pradat PF, Lope J, Vourc'h P, Blasco H, Corcia P. Primary lateral sclerosis: clinical, radiological and molecular features. Rev Neurol 2021;2021:S0035-3787(21)00592-0.
41. Verstraete E, Turner MR, Grosskreutz J, Filippi M, Benatar M. Mind the gap: the mismatch between clinical and imaging metrics in ALS. Amyotroph Lateral Scler Frontotemporal Degener. 2015;16:524–9.
42. Turner MR, Barohn RJ, Corcia P, Fink JK, Harms MB, Kiernan MC, et al. Primary lateral sclerosis: consensus diagnostic criteria. J Neurol Neurosurg Psychiatry. 2020; 91:373–7.,
43. Christidi F, Karavasilis E, Rentzos M, Velonakis G, Zouvelou V, Xirou S, et al. Hippocampal pathology in amyotrophic lateral sclerosis: selective vulnerability of subfields and their associated projections. Neurobiol Aging. 2019;84:178–88.
44. Douaud G, Smith S, Jenkinson M, Behrens T, Johansen-Berg H, Vickers J, et al. Anatomically related grey and white matter abnormalities in adolescent-onset schizophrenia. Brain. 2007;130:2375–86.
45. Good CD, Johnsrude IS, Ashburner J, Henson RN, Friston KJ, Frackowiak RS. A voxel-based morphometric study of ageing in 465 normal adult human brains. Neuroimage. 2001;14:21–36.
46. Diedrichsen J, Balsters JH, Flavell J, Cussans E, Ramnani N. A probabilistic MR atlas of the human cerebellum. Neuroimage. 2009;46:39–46.

47. Schuster C, Elamin M, Hardiman O, Bede P. The segmental diffusivity profile of amyotrophic lateral sclerosis associated white matter degeneration. Eur J Neurol. 2016; 23:1361–71.
48. Smith SM, Jenkinson M, Johansen-Berg H, Rueckert D, Nichols TE, Mackay CE, et al. Tract-based spatial statistics: voxelwise analysis of multi-subject diffusion data. Neuroimage. 2006;31:1487–505.
49. Romero JE, Coupé P, Giraud R, Ta V-T, Fonov V, Park MTM, et al. CERES: a new cerebellum lobule segmentation method. Neuroimage. 2017;147:916–24.
50. Park MTM, Pipitone J, Baer LH, Winterburn JL, Shah Y, Chavez S, et al. Derivation of high-resolution MRI atlases of the human cerebellum at 3T and segmentation using multiple automatically generated templates. Neuroimage. 2014;95:217–31.
51. Schoch B, Dimitrova A, Gizewski ER, Timmann D. Functional localization in the human cerebellum based on voxelwise statistical analysis: a study of 90 patients. Neuroimage. 2006;30:36–51.
52. Guell X, Gabrieli JDE, Schmahmann JD. Triple representation of language, working memory, social and emotion processing in the cerebellum: convergent evidence from task and seed-based resting-state fMRI analyses in a single large cohort. Neuroimage. 2018;172:437–49.
53. Kansal K, Yang Z, Fishman AM, Sair HI, Ying SH, Jedynak BM, et al. Structural cerebellar correlates of cognitive and motor dysfunctions in cerebellar degeneration. Brain. 2017;140:707–20.
54. Palesi F, Tournier J-D, Calamante F, Muhlert N, Castellazzi G, Chard D, et al. Contralateral cerebello-thalamo-cortical pathways with prominent involvement of associative areas in humans *in vivo*. Brain Struct Funct. 2015;220:3369–84.
55. Palesi F, De Rinaldis A, Castellazzi G, Calamante F, Muhlert N, Chard D, et al. Contralateral cortico-ponto-cerebellar pathways reconstruction in humans *in vivo*: implications for reciprocal cerebro-cerebellar structural connectivity in motor and non-motor areas. Sci Rep. 2017;7:12841.
56. Chipika RH, Finegan E, Li Hi Shing S, McKenna MC, Christidi F, Chang KM, et al. “Switchboard” malfunction in motor neuron diseases: selective pathology of thalamic nuclei in amyotrophic lateral sclerosis and primary lateral sclerosis. Neuroimage Clin. 2020;27:102300.
57. Chipika RH, Siah WF, Shing SLH, Finegan E, McKenna MC, Christidi F, et al. MRI data confirm the selective involvement of thalamic and amygdalar nuclei in amyotrophic lateral sclerosis and primary lateral sclerosis. Data Brief. 2020;32:106246.
58. Coon EA, Whitwell JL, Jack CR, Josephs KA. Primary lateral sclerosis as progressive supranuclear palsy: diagnosis by diffusion tensor imaging. Mov Disord. 2012;27:903–6.
59. Bharti K, Khan M, Beaulieu C, Graham SJ, Briemberg H, Frayne R, et al. Involvement of the dentate nucleus in the pathophysiology of amyotrophic lateral sclerosis: a multi-center and multi-modal neuroimaging study. Neuroimage Clin. 2020;28:102385.
60. McKenna MC, Chipika RH, Li Hi Shing S, Christidi F, Lope J, Doherty MA, et al. Infratentorial pathology in frontotemporal dementia: cerebellar grey and white matter alterations in FTD phenotypes. J Neurol. 2021;268: 4687–97.,
61. Bede P, Iyer PM, Schuster C, Elamin M, Mclaughlin RL, Kenna K, et al. The selective anatomical vulnerability of ALS: ‘disease-defining’ and ‘disease-defying’ brain regions. Amyotroph Lateral Scler Frontotemporal Degener. 2016; 17:561–70.
62. Bede P, Elamin M, Byrne S, McLaughlin RL, Kenna K, Vajda A, et al. Patterns of cerebral and cerebellar white matter degeneration in ALS. J Neurol Neurosurg Psychiatry. 2015;86:468–70.
63. Feron M, Couillandre A, Mseddi E, Termoz N, Abidi M, Bardinet E, et al. Extrapyramidal deficits in ALS: a combined biomechanical and neuroimaging study. J Neurol. 2018;265:2125–36.
64. Abidi M, de Marco G, Grami F, Termoz N, Couillandre A, Querin G, et al. Neural Correlates of Motor Imagery of Gait in Amyotrophic Lateral Sclerosis. J Magn Reson Imaging. 2021;53:223–33.
65. Finegan E, Li Hi Shing S, Chipika RH, Doherty MA, Hengeveld JC, Vajda A, et al. Widespread subcortical grey matter degeneration in primary lateral sclerosis: a multimodal imaging study with genetic profiling. Neuroimage Clin. 2019;24:102089.
66. Grollemund V, Chat GL, Secchi-Buhour M-S, Delbot F, Pradat-Peyre J-F, Bede P, et al. Development and validation of a 1-year survival prognosis estimation model for Amyotrophic Lateral Sclerosis using manifold learning algorithm UMAP. Sci Rep. 2020;10: 13378.
67. Bede P, Murad A, Hardiman O. Pathological neural networks and artificial neural networks in ALS: diagnostic classification based on pathognomonic neuroimaging features. J Neurol. 2021.doi: 10.1007/s00415-021-10801-5.
68. Grollemund V, Le Chat G, Secchi-Buhour M-S, Delbot F, Pradat-Peyre J-F, Bede P, et al. Manifold learning for amyotrophic lateral sclerosis functional loss assessment: development and validation of a prognosis model. J Neurol. 2021;268:825–50.
69. Bede P, Murad A, Lope J, Li Hi Shing S, Finegan E, Chipika RH, et al. Phenotypic categorisation of individual subjects with motor neuron disease based on radiological disease burden patterns: a machine-learning approach. J Neurol Sci. 2021;432:120079.
70. Querin G, El Mendili M-M, Bede P, Delphine S, Lenglet T, Marchand-Pauvert V, et al. Multimodal spinal cord MRI offers accurate diagnostic classification in ALS. J Neurol Neurosurg Psychiatry. 2018;89:1220–1.
71. Clark MG, Smallwood Shoukry R, Huang CJ, Danielian LE, Bageac D, Floeter MK. Loss of functional connectivity is an early imaging marker in primary lateral sclerosis. Amyotrop Lateral Scler Frontotemporal Degener. 2018;19:562–8.
72. Floeter MK, Mills R. Progression in primary lateral sclerosis: a prospective analysis. Amyotroph Lateral Scler. 2009;10:339–46.
73. Tahedl M, Li Hi Shing S, Finegan E, Chipika RH, Lope J, Hardiman O, et al. Propagation patterns in motor neuron diseases: individual and phenotype-associated disease-burden trajectories across the UMN-LMN spectrum of MNDs. Neurobiol Aging. 2022;109:78–87.
74. Menke RAL, Proudfoot M, Talbot K, Turner MR. The two-year progression of structural and functional cerebral MRI in amyotrophic lateral sclerosis. Neuroimage Clin. 2018;17:953–61.
75. Bede P, Hardiman O. Longitudinal structural changes in ALS: a three time-point imaging study of white and gray matter degeneration. Amyotroph Lateral Scler Frontotemporal Degener. 2018;19:232–41.
76. Chipika RH, Finegan E, Li Hi Shing S, Hardiman O, Bede P. Tracking a fast-moving disease: longitudinal markers, monitoring, and clinical trial endpoints in ALS. Front Neurol. 2019;10:229.
77. Abidi M, de Marco G, Couillandre A, Feron M, Mseddi E, Termoz N, et al. Adaptive functional reorganization in amyotrophic lateral sclerosis: coexisting degenerative and compensatory changes. Eur J Neurol. 2020;27:121–8.
78. Proudfoot M, Bede P, Turner MR. Imaging cerebral activity in amyotrophic lateral sclerosis. Front Neurol. 2018;9:1148.

79. Bede P, Bogdahn U, Lope J, Chang KM, Xirou S, Christidi F, et al. Degenerative and regenerative processes in amyotrophic lateral sclerosis: motor reserve, adaptation and putative compensatory changes. Neural Regen Res. 2021;16:1208–9.
80. Li Hi Shing S, Lope J, McKenna MC, Chipika RH, Hardiman O, Bede P, et al. Increased cerebral integrity metrics in poliomyelitis survivors: putative adaptation to longstanding lower motor neuron degeneration. J Neurol Sci. 2021;424:117361.
81. Li Hi Shing S, Lope J, Chipika RH, Hardiman O, Bede P. Imaging data indicate cerebral reorganisation in poliomyelitis survivors: possible compensation for longstanding lower motor neuron pathology. Data Brief. 2021;38:107316.
82. Nasseroleslami B, Dukic S, Broderick M, Mohr K, Schuster C, Gavin B, et al. Characteristic increases in EEG connectivity correlate with changes of structural MRI in amyotrophic lateral sclerosis. Cereb Cortex. 2019;29:27–41.
83. Dukic S, McMackin R, Buxo T, Fasano A, Chipika R, Pinto-Grau M, et al. Patterned functional network disruption in amyotrophic lateral sclerosis. Hum Brain Mapp. 2019;40:4827–42.
84. Steinacker P, Feneberg E, Weishaupt J, et al. Neurofilaments in the diagnosis of motoneuron diseases: a prospective study on 455 patients. J Neurol Neurosurg Psychiatry 2016;87:12–20.
85. Devos D, Moreau C, Kyheng M, Garçon G, Rolland AS, Blasco H, et al. A ferroptosis-based panel of prognostic biomarkers for Amyotrophic Lateral Sclerosis. Sci Rep. 2019;9:2918.
86. Blasco H, Patin F, Descat A, Garçon G, Corcia P, Gelé P, et al. A pharmaco-metabolomics approach in a clinical trial of ALS: identification of predictive markers of progression. PLoS One. 2018;13:e0198116.
87. Diedrichsen J. A spatially unbiased atlas template of the human cerebellum. Neuroimage. 2006;33:127–38.